Response to Reviewer CC1

Title: Two-dimensional Differential-form of Distributed Xinanjiang Model

Authors: Jianfei Zhao, Zhongmin Liang*, Vijay P. Singh, Taiyi Wen, Yiming Hu, Binquan Li, Jun Wang

Manuscript ID: hess-2024-377

Thank you very much for your interest and valuable suggestions regarding our manuscript. All your comments have been carefully addressed, and a point-by-point response is provided below.

For better readability, the point-by-point response is formatted as follows:

- Reviewer's comments are shown in black
- Authors' responses are shown in blue
- Revisions to be incorporated in the revised manuscript are highlighted in red

Overall comments:

In the study, a two-dimensional differential-form of distributed Xinanjiang Model was developed. This work is interesting and valuable. Through applying the proposed model, a good performance is achieved. But there are still some points that should be explained or revised before publication.

We appreciate your recognition of both the value of our work and the performance achieved by our proposed model. We have carefully considered all of your comments and responded to them in the subsequent specific comments section. We hope that these changes could effectively address your concerns.

Specific comments:

1. There are many parameters in the proposed TDD-XAJ model, the authors should state the method for parameter calibration. If the calibration is done as stated in Line 432 (calibrated manually), a lot of work should done.

Thanks for your comments. The TDD-XAJ model comprises 15 parameters, which is one parameter more than the original lumped Xinanjiang model (Zhao et al., 2023), with 11 hydrological parameters for runoff generation and 4 parameters (2 hydrological and 2 hydraulic) for runoff concentration. The two hydraulic parameters are surface roughness coefficient (n_s) and channel roughness coefficient (n_c). For n_s, values are assigned based on the land use type of each grid cell, with different land uses corresponding to different roughness coefficients, which are derived from existing literature (Miao et al., 2016; Perrini et al., 2024). For n_c, values are obtained from a roughness coefficient table for river channels (Arcement and Schneider, 1989). Since this manuscript primarily focuses on the theoretical aspects of the TDD-XAJ model, we adopted uniform watershed-scale parameter values to simplify the research, thereby keeping the calibration workload manageable.

To determine spatially heterogeneous hydrological parameters, the process is generally based on spatially quantified data of watershed physical characteristics. This work is primarily carried out in two ways:

(1) **Lookup table-based method**. Parameters are determined from tables based on watershed physical attributes. Specifically, the ratio of the impervious area (A_{imp}) and coefficient of deep soil layer evapotranspiration (c) are determined according to land use types (Yao et al., 2012), while the determination of tension water storage capacity curve exponent (b) and free water storage capacity curve exponent (ex) are assigned based on soil types.

(2) **Physical meaning-based method**. Parameter values are calculated using quantitative watershed physical characteristics according to the physical meaning of the parameters. Specifically:

a. Tension water storage capacity of the upper, lower, and deep soil layer (W_{um}, W_{lm}, and W_{dm}). The summation of W_{um}, W_{lm}, and W_{dm} represents the tension water capacity of the entire soil layer (W_m), which can be calculated by the difference between field capacity (θ_f) and residual water content (θ_r) and multiplying the soil layer depth (D_s, with the unit of mm). Subsequently, two watershed-scale uniform coefficients (K_{um} and K_{lm}) and their derived value (1-K_{um}-K_{lm}) are used to divide W_m into W_{um}, W_{lm}, and W_{dm} accordingly (Yao et al., 2012).

b. Free water storage capacity (S_m). S_m usually represents the capacity of free water capacity in the humus layer. It is calculated by multiplying humus layer depth (D_h, with the unit of mm) and the difference between saturated water content (θ_s) and field capacity (θ_f), as also described by Yao et al. (2012).

c. Interflow and groundwater outflow coefficient (K_i and K_g). K_i and K_g represent the outflow rate of interflow and groundwater. The method for determining these parameters involves converting the storage of interflow and groundwater linear reservoir to corresponding saturated water depth, based on the hillslope storage-discharge theory and steady-state assumptions. These are then multiplied by the slope gradient and the saturated hydraulic conductivity of the upper (representing interflow) and lower (representing groundwater) layers, using the kinematic wave assumption (Tong, 2022). K_i and K_g are finally expressed as the ratios of corresponding flow distance in the time interval of input forces to the slope length.

d. Interflow and groundwater storage recession coefficient (C_i and C_g). C_i and C_g represent the time delay for interflow and groundwater runoff as they travel from specific locations on the slope to the river channel. These parameters are determined based on the theory of spatially distributed unit hydrograph (Maidment et al., 1996). The grid cells that form the flow path extending from specific locations on the slope to the river channel is first identified using GIS. Then, using the kinematic wave assumption, the flow velocity of interflow and groundwater runoff through each grid cell is computed based on the saturated hydraulic conductivity of the upper and lower layers and the slope gradient. Finally, the time taken for flow through each grid cell is accumulated, and the parameters for each grid cell are derived using theoretical conversion formulas (Tong, 2022).

e. The remaining parameter is coefficient of potential evapotranspiration to pan evaporation (K_e), which is usually treated as watershed-scale uniform parameters.

The primary data used to determine spatially heterogeneous model parameters include soil physical and hydraulic properties, slope gradient, and land use. These can be obtained from open-source datasets, such as Harmonized World Soil Database v2.0 (HWSD v2.0) (FAO and IIASA, 2023), China dataset of soil properties for land surface modelling version 2 (CSDLv2) (Shi et al., 2025), and Global land cover mapping at 30m resolution (GlobeLand30) (Chen et al., 2015). In addition to manual calibration, uniform watershed-scale parameters or coefficients can also be determined using automated optimization algorithms, such as the Covariance Matrix Adaptation Evolution Strategy (CMA-ES) (Hansen et al., 2003). We plan to integrate this approach into the TDD-XAJ model in future developments.

2. Line 423, Daily scale hydrological data were used in the study. I think the constructed model can be used for flood events simulation. Why don't you attempt to use sub-daily hydrological data?

The governing equations of the TDD-XAJ model are transformed into a system of ordinary differential equations after spatial discretization. The model can generate both instantaneous and time-averaged values of state variables and fluxes over a specified time interval through numerical integration, offering flexibility in model temporal resolution. As a result, the model is well-suited for daily-scale continuous simulations as well as flood event-based simulations (which usually use sub-daily data), as you mentioned in your comment. We have collected sufficiently long daily-scale hydrological data (spanning 2007-2019, totaling 13 year), but we did not gather enough sub-daily scale hydrological data. Consequently, this study relies on daily-scale hydrological data. In future work, we plan to collect additional sub-daily data as a foundation for exploring flood events simulation.

3. Line 456, the spatial distribution of the Oi has been zoomed into the upper left corner. I suggest the authors provide the spatial distribution of the entire area, and then zoom the upper left corner.

Thank you for your suggestion. This visualization approach will allow us to present the full spatial distribution of the O_i, ensuring data integrity while also highlighting the differences in the upper left corner. As reviewer RC1 noted, the contrast between Figures 7b and 7d was unclear, and your recommended visualization approach effectively addresses this issue. As you suggested, the revised Figure 7 is shown below:

"Line 452-457:

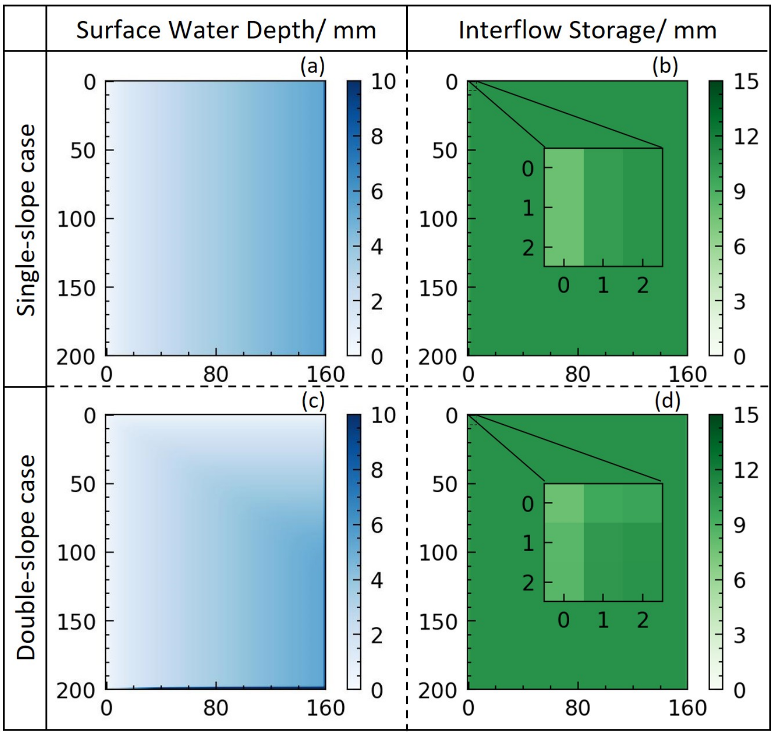

Figure 7. The spatial distribution of surface water depth (h_s) and interflow storage (O_i) on the left-side hillslope of both single-slope (a-b) and double-slope (c-d) synthetic V-catchment test cases at the 60 minute mark. The state variable distributions shown are simulated using two-dimensional (2D) slope concentration methods. The corresponding results of 1D methods are identical to those obtained from the single-slope case simulated with 2D methods, regardless of the test case used. For a clear comparison, the spatial distribution of O_i in the upper left corner has been zoomed."

4. In Table 2, average MAE statistics of model fluxes for a total of 500 parameter sets are provided using loosely coupled model. But the reference is the fully-coupled model. This cannot illustrate the better performance of fully-coupled model.

The main difference between the loosely-coupled (LC) and fully-coupled (FC) model lies in their numerical implementation frameworks. In the LC model, the difference-form equations for runoff generation from the original lumped XAJ model are directly adopted, which are derived based on the time interval of input force (ΔT). However, for runoff concentration, the LC model uses differential-form equations; consequently, the generated runoff components (surface runoff, interflow, and groundwater runoff) are averaged over ΔT to determine the input intensities for the following runoff concentration equations. In contrast, the FC model adopts differential-form equations for both runoff generation and runoff concentration, solving both processes simultaneously as a system of ordinary differential equations (ODEs). In the FC model, the total amount of input force, rather than further calculated runoff components, is averaged over ΔT.

We compared the LC model and FC model on single-slope and double-slope synthetic V-shaped watershed test cases using the same 500 parameter sets. An analytical solution exists for the total amount of surface runoff (R_S^*). When the ΔT was set to 90 minutes, the average mean absolute error (MAE) for R_S^* in the LC model was 4.57 mm, compared to 2.84×10^{-4} mm for the FC model. As ΔT was reduced to 45 minutes and 15 minutes, the average MAE for R_S^* in the LC model decreased to 1.21 mm and 0.14 mm, respectively; however, these errors remain significantly higher than those of the FC model.

For hillslope or channel outflow, no analytical solution is available, which makes direct comparison challenging. To address this, we evaluated the convergence of the LC model by progressively reducing ΔT. The difference-form runoff generation equations used by the LC model have first-order temporal accuracy, and the FC model provides a high-order approximation of the analytical solution. Theoretically, as ΔT decreases, the results of the LC model should converge to those of the FC model. We used MAE to evaluate the consistency between the hillslope and channel outflow hydrographs simulated by the FC and LC models. Our numerical experiment showed that the average MAE decreases as ΔT is reduced, indicating that the LC model's results converge toward those of the FC model. Furthermore, significant numerical errors could be observed in the LC model (ΔT=90 minutes), whether benchmarked against the LC model (ΔT=15 minutes) or the FC model (ΔT=90 minutes). In the single-slope test case, when using the LC model (ΔT=15 minutes) as the benchmark, the average MAE for channel and hillslope outflow are 1.82 mm and 1.64 mm, respectively, whereas when using the FC model (ΔT=90 minutes) as the benchmark, the average MAE are 1.85 mm and 1.68 mm. In the double-slope test case, when using the LC model (ΔT=15 minutes) as the benchmark, the average MAE for channel and hillslope outflow are 1.83 mm and 1.68 mm, respectively, while benchmarked against the FC model (ΔT=90 minutes) yields average MAE of 1.87 mm and 1.72 mm. Additionally, the outflow hydrograph simulated by the LC model exhibits non-physical steady states and inflection points, which indicate its potential limitations in capturing transient behaviors.

Overall, when an analytical solution is available, the error of the LC model is several orders of magnitude higher than that of the FC model. In cases without an analytical solution, as ΔT decreases, results of the LC model converge to those of the FC model. Furthermore, non-physical steady states and inflection points are observed in the hydrograph simulated by the LC model. Consequently, the FC model is considered to performs better in numerical simulations.

5. Line 505, the 2 values cannot be found in Table 2.

Thank you for pointing this out. To keep Table 2 concise, we initially approximated the very small values (4.19×10^{-3} and 2.84×10^{-4}) as 0 and used "~0.00" to maintain alignment in the column. The exact values are provided in the following lines for clarity. To avoid any misunderstanding, we have now included the values in scientific notation directly in Table 2. The revised Table is shown below:

"Line 500:

Table 2. MAE statistics of model fluxes in numerical implementation comparison experiment.

Model	ΔT (min)	Statistics	MAE (mm)	MAE (m^3/s)			
			R_s^*	Hillslope outflow		Channel outflow	
				Single-slope	Double-slope	Single-slope	Double-slope
Loosely-coupled	90	Max	5.93	2.19	2.20	2.01	2.06
		Average	4.57	1.85	1.87	1.68	1.72
	45	Max	2.01	1.60	1.62	1.31	1.41
		Average	1.21	0.81	0.82	0.70	0.73
	15	Max	0.33	0.56	0.61	0.36	0.39
		Average	0.14	0.16	0.17	0.11	0.12
Fully-coupled	90	Max	4.19×10^{-3}	—[a]	—	—	—
		Average	2.84×10^{-4}	—	—	—	—

a. The results of the fully-coupled model are used as references to calculate the MAE values for hillslope and channel outflow, so the corresponding value is empty."

6. The simulation in the Tunxi watershed was only compared with 1 previous study in the same watershed. Is it possible to compare the results with previous research using other lumped or distributed models in the same or adjacent watershed?

Thank you for your suggestion. For the present study, we focused on comparing our simulation in the Tunxi watershed with a well-documented previous study in the same area to ensure consistency in benchmark data. The primary focus of this study is on the theoretical aspect of the TDD-XAJ model. We acknowledge that further validation, including comparisons with other models, remains necessary. However, difficulties in data availability, model structure, and parameterization among studies made such a comparison challenging at this stage. While inter-model comparison was not implemented, validation targeting a hydrological station within the Tunxi Watershed was executed to strengthen model performance evaluation.

We introduced the Yuetan hydrological station—a station within the Tunxi watershed (Figure 5), and compared its simulation results with observed data. Details of performance metrics are provided in Table 4. As shown in Table 4, the average values of the Nash-Sutcliffe efficiency (NSE), Kling-Gupta efficiency (KGE), the absolute flood volume relative error (|FVRE|), and the coefficient of determination (R^2) for Yuetan station (across all years) are 0.83, 0.78, 6.2%, and 0.86, respectively. The corresponding values for Tunxi station are 0.87, 0.80, 6.7%, and 0.90. In summary, these metrics indicate that the TDD-XAJ model provides robust streamflow simulations at both stations in the Tunxi watershed. The revisions to be implemented are detailed below:

"Line 421:

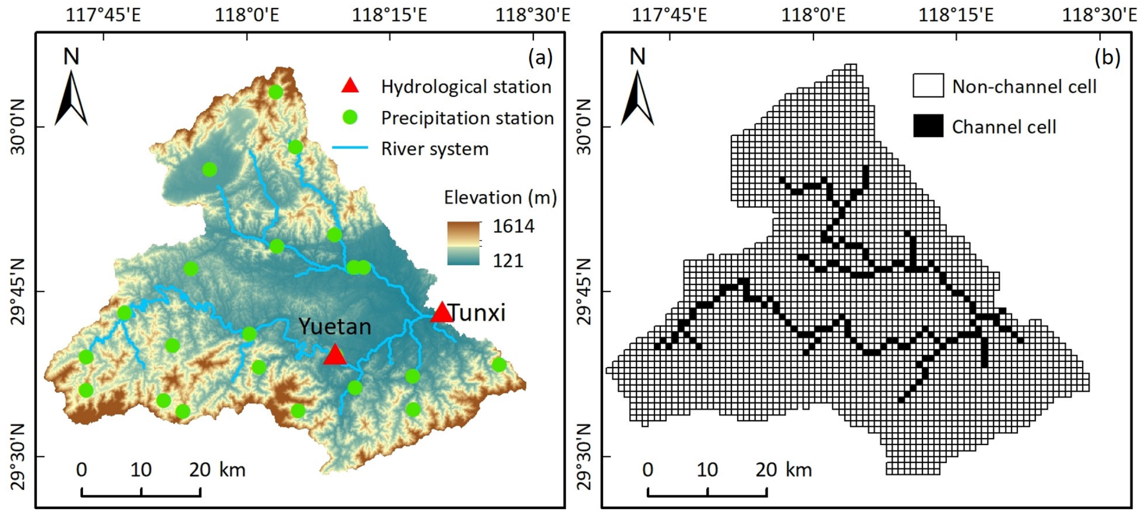

Figure 5. Location and gauging station distribution of the Tunxi watershed (a), and the spatial discretization of the watershed, including channel and non-channel cells (b)."

"Line 553-560:

Table 4. Annually evaluated simulation performance metrics of the TDD-XAJ model in the Tunxi watershed.

Period	Year	Tunxi				Yuetan			
		NSE	KGE	FVRE(%)	R^2	NSE	KGE	FVRE(%)	R^2
Calibration	2008	0.94	0.91	-8.26	0.94	0.90	0.89	-1.33	0.90
	2009	0.88	0.90	-6.95	0.88	0.82	0.80	-16.43	0.83
	2010	0.85	0.78	-16.88	0.90	0.82	0.78	-18.99	0.87
	2011	0.89	0.78	7.53	0.89	0.78	0.76	-3.46	0.80
	2012	0.82	0.84	-7.64	0.83	0.74	0.80	-5.97	0.74
	2013	0.87	0.80	-10.75	0.92	0.88	0.79	-3.99	0.92
	2014	0.88	0.79	0.20	0.91	0.84	0.75	0.72	0.87
Validation	2015	0.85	0.77	-9.92	0.92	0.85	0.80	-8.48	0.88
	2016	0.88	0.78	-6.92	0.92	0.86	0.79	-4.37	0.89
	2017	0.88	0.76	1.62	0.92	0.84	0.72	4.66	0.86
	2018	0.87	0.77	1.58	0.89	0.87	0.78	-2.75	0.90
	2019	0.85	0.74	-2.24	0.89	0.79	0.74	-3.70	0.81

For the outlet station of Tunxi watershed, Table 4 indicates that the values of the FVRE metric are all within ±20 %. The absolute values of the FVRE (|FVRE|) averaging 8.3 % for the calibration period and 4.5 % for the validation period. In terms of hydrograph evaluation, the average values of NSE and KGE are 0.88 and 0.83 for the calibration period and 0.87 and 0.76 for the validation period, which is slightly better for the calibration period than for the validation period. The minimum value of R^2 is 0.83 for all years, and the average value for all years is 0.90. In a direct comparison, Tong (2022) conducted a similar daily simulation in the same watershed using the GXAJ model, reporting average NSE and |FVRE| values of 0.85 and 11.0% between 2008 and 2017, respectively. In contrast, the TDD-XAJ model achieved average values of 0.87 for NSE and 7.7% for |FVRE| in the same period. For the Yuetan station within Tunxi watershed, Table 4 shows that FVRE metric values remain within ±20 %. The average (|FVRE|) is 7.3 % and 4.8 % for the calibration and validation periods, respectively. Meanwhile, the average value of NSE is 0.82 for the calibration period and 0.84 for the validation period, and the average KGE is 0.80 and 0.77 for calibration period and validation period, respectively. Across all years, the average R^2 reaches 0.86."

"Line 563-566:

Fig. 9 provides an example of the simulated hydrograph at Tunxi and Yuetan station of the TDD-XAJ model in 2008.

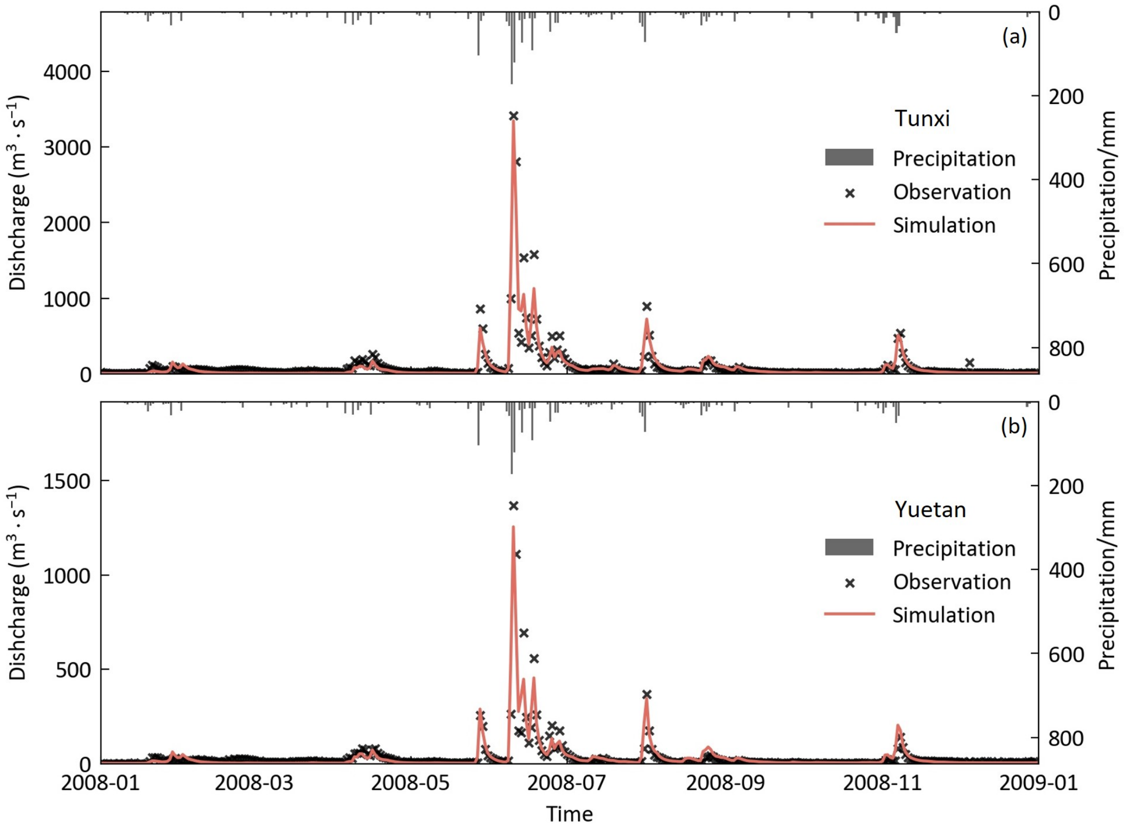

Figure 9. The simulated hydrograph at Tunxi (a) and Yuetan (b) station of the Tunxi watershed in 2008 using the TDD-XAJ model."

References mentioned in the response

Arcement, G. J. and Schneider, V. R.: Guide for selecting manning's roughness coefficients for natural channels and flood plains, 2339, https://doi.org/10.3133/wsp2339, 1989.

Chen, J., Chen, J., Liao, A., Cao, X., Chen, L., Chen, X., He, C., Han, G., Peng, S., Lu, M., Zhang, W., Tong, X., and Mills, J.: Global land cover mapping at 30m resolution: A POK-based operational approach, ISPRS-J. Photogramm. Remote Sens., 103, 7-27, https://doi.org/10.1016/j.isprsjprs.2014.09.002, 2015.

FAO and IIASA: Harmonized world soil database (version 2.0) [dataset], https://www.fao.org/soils-portal/data-hub/soil-maps-and-databases/harmonized-world-soil-database-v20/en/, 2023.

Hansen, N., Müller, S. D., and Koumoutsakos, P.: Reducing the Time Complexity of the Derandomized Evolution Strategy with Covariance Matrix Adaptation (CMA-ES), Evol. Comput., 11, 1-18, https://doi.org/10.1162/106365603321828970, 2003.

Maidment, D. R., Olivera, F., Calver, A., Eatherall, A., and Fraczek, W.: Unit hydrograph derived from a spatially distributed velocity field, Hydrol. Process., 10, 831-844, https://doi.org/10.1002/(SICI)1099-1085(199606)10:6<831::AID-HYP374>3.0.CO;2-N, 1996.

Miao, Q., Yang, D., Yang, H., and Li, Z.: Establishing a rainfall threshold for flash flood warnings in China's mountainous areas based on a distributed hydrological model, J. Hydrol., 541, 371-386, https://doi.org/10.1016/j.jhydrol.2016.04.054, 2016.

Perrini, P., Cea, L., Chiaravalloti, F., Gabriele, S., Manfreda, S., Fiorentino, M., Gioia, A., and Iacobellis, V.: A runoff-on-grid approach to embed hydrological processes in shallow water models, Water Resour. Res., 60, e2023WR036421, https://doi.org/10.1029/2023WR036421, 2024.

Shi, G., Sun, W., Shangguan, W., Wei, Z., Yuan, H., Li, L., Sun, X., Zhang, Y., Liang, H., Li, D., Huang, F., Li, Q., and Dai, Y.: A China dataset of soil properties for land surface modelling (version 2, CSDLv2), Earth Syst. Sci. Data, 17, 517-543, https://doi.org/10.5194/essd-17-517-2025, 2025.

Tong, B.: Fine-scale rainfall-runoff processes simulation using grid Xinanjiang (grid-XAJ) model, Hohai University, Nanjing, Jiangsu, 2022.

Yao, C., Li, Z., Yu, Z., and Zhang, K.: A priori parameter estimates for a distributed, grid-based Xinanjiang model using geographically based information, J. Hydrol., 468-469, 47-62, https://doi.org/10.1016/j.jhydrol.2012.08.025, 2012.

Zhao, J., Duan, Y., Hu, Y., Li, B., and Liang, Z.: The numerical error of the Xinanjiang model, J. Hydrol., 619, 129324, https://doi.org/10.1016/j.jhydrol.2023.129324, 2023.